

A New Methodology for Classifying QRS Morphology in ECG Signals

Wesley L. Caldas
Dept. of Computer Science
Federal University of Ceará
Fortaleza, Brazil
wesleylc@lia.com.br

João Paulo V. Madeiro
Dept. of Computer Science
Federal University of Ceará
Fortaleza, Brazil
jpaulo.vale@dc.ufc.br

César Lincoln C. Mattos
Dept. of Computer Science
Federal University of Ceará
Fortaleza, Brazil
cesarlincoln@dc.ufc.br

João Paulo P. Gomes
Dept. of Computer Science
Federal University of Ceará
Fortaleza, Brazil
jpaulo@dc.ufc.br

Abstract—The electrocardiogram (ECG) is a non-invasive method to detect cardiovascular diseases (CVD), the most common cause of death in the world. The recognition of heartbeat morphologies present in the ECG signal is an effective way to detect CVDs prematurely. Many approaches were developed for this purpose, such as the use of Wavelets, High Order Statistics (HOS), Local Binary Patterns (LBP), Random Projection, Fiducial points, and Hermite Polynomials. Unfortunately, most parts of these approaches suffer from the high variability of ECG signal features and conditions. Also, it is common to use more than one of them simultaneously, which makes it hard to infer the contributions of each one. This work presents a new robust methodology to extract features for heartbeat morphology classification. Moreover, we introduce new labels for a small set of morphologies present in MIT-BIH Arrhythmia database, taking into account only the QRS complex (the 3 more representative waves of a heartbeat) instead of the whole heartbeat. We evaluate each approach in isolation and the results show that our method outperforms other well-known strategies.

Index Terms—ECG signal, QRS morphology, feature extraction, prediagnosis.

I. INTRODUCTION

Cardiovascular diseases (CVD) are the most common cause of death globally, producing immense health and economic burdens. According to the World Health Organization (WHO): “People with cardiovascular disease or who are at high cardiovascular risk need early detection and management using counseling and medicines, as appropriate”. Despite the continuous advance of medicine, the ECG continues to be a crucial non-invasive tool to detect CVD. As a result, the ECG data analysis has become a significant field of study. Most of the useful information within ECG data is present on the intervals and amplitudes which characterizes the significant regions (wave peaks and boundaries) that compose the standard cardiac cycle (heartbeat) [14]. These characteristic waves occur due to electrical changes caused by depolarization/repolarization cycles inside the heart. Depolarizations result in atrial contractions, which are associated with P waves, and ventricular contractions, which are associated to the QRS complex. Polarization results in the return of the ventricular mass to the relaxation state, producing the T waves. The junction of all these waves forms the PQRST cycle.

During, PQRST complex analysis (shape, duration, interval patterns and etc.) has received much attention from the re-

search community, resulting in significant advances in many areas like disease diagnosis [12, 17], heartbeat segmentation [14], and heartbeat delineation [1, 14, 25]. Incidentally, the QRS complex is the most characteristic waveform of the PQRST cycle, presenting, in general, a higher amplitude than the other waves.

The morphological structure (curve shape) of the QRS complex is one of the main features of a heartbeat and may indicate many types of diseases or disorders [2]. In [7], the authors have demonstrated that morphologies serve to robustly predict long-term mortality in Left Ventricular Pacing (LVP) patients. Another important task solved by recognizing morphologies is detecting arrhythmias [22, 23]. Furthermore, the correct identification of the heartbeat shape helps on prognostics: patients that present non-LBBB (Left Bundle Branch Block) morphology commonly do not respond well for specific treatments, like Cardiac Resynchronization Therapy (CRT)[20]. Finally, the QRS morphology is a better indicator than the QRS duration for longterm survival, since people with LBBB morphology present less ischaemic cardiomyopathy and atrial fibrillation [9].

The importance of the QRS morphology for diagnostics/prognostics motivated many approaches to recognize such shapes, such as the use of Wavelets [13, 14], Higher-Order Statistics (HOS) [3, 18, 19], Random Projection [6], Fiducial points of the heartbeat [17], and Hermite Polynomial [10]. Unfortunately, most of these features do not perform well when mismatch data is present, i.e., they need the test instances to be similar to the training set. Besides, since most parts of these methodologies are evaluated in conjunction with other approaches, it is hard to determine the real efficiency of each one.

This work introduces a new approach to extract features from the QRS complex based on the so-called mathematical models [5] and presents a comparative study with all methodologies previously mentioned. We named our approach as feature extraction via residuals from modeling with composition of mathematical functions (RCMF). From five mathematical models built upon three functions (Rayleigh, Gaussian, and Mexican-hat), we create a morphological descriptor related only to the shape of each beat, instead of the amplitude and duration of its waves.

To validate our approach, we consider the well-known public dataset MIT-BIH Arrhythmia database. Typically, this dataset contains five classes of morphologies representing arrhythmias: N corresponding to any heartbeat which does not pertain to other categories, S, supraventricular ectopic beat, V, ventricular ectopic beat, F, fusion beat, Q, unknown beat. Different from the previous works, we do not focus on classifying the entire heartbeat morphology, but only on the QRS complexes morphology. This classification is already made implicitly in the other approaches, which generally extract the QRS complex, apply its descriptor and then classify the complete cardiac cycle. However, to ascertain the describing ability of the QRS complex provided by each method, we will only classify its morphologies. For this purpose, we use a synthetic ECG simulator to produce artificial ECG data for the four typical morphologies qRs, RS, rRs and QS to constitute our training set. After that, we select a small portion of the MIT-BIH dataset (14 subjects) whose QRS complexes contain the four types of morphologies qRs, RS, rRs, QS and apply an algorithm to detect QRS complex. The full set of beats is labeled by a specialist concerning each morphology and serves as our validation set. The performed experimental results show that our methodology outperforms other well-know feature extraction methodologies available in the literature.

The remaining of this paper is organized as follows. Section II presents the methodology applied for generating artificial signals and the common features applied for heartbeat classification. Section III shows the proposed approach based on mathematical models. Section IV details the corresponding related work within the literature. Section V describes the training/test datasets applied in this work. Description of the experiments and results using the proposed labels for MIT-BIH can be seen in Section VI. Finally, Section VII presents our conclusions and comments for future works.

II. ECG DATA SIMULATION

The QRS complex presents a high variability, since both the shape and the amplitude of the waves are governed by multiple individual factors, like the shape/position of the heart and the presence and nature of pathologies, among others [11]. As a result, the QRS complex can be categorized depending on the shape of its waves. In this study, we use the 4 common variations (qRs, RS, QS and rRs), presented in Fig. 1. Table I presents the average of corresponding wavelengths and amplitudes.

TABLE I: Wave amplitude/duration for QRS waves [11].

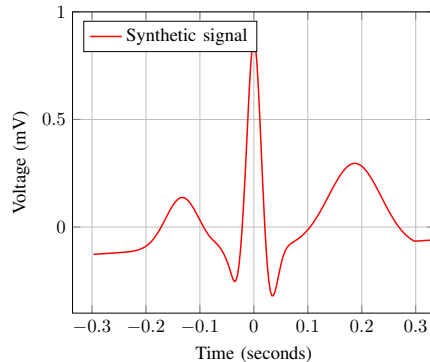
Type of Wave	ECG normal values	
	Amplitude(mV)	Duration(Seconds)
Q	0.00 - 0.30	0.06 - 0.10
R	0.60 - 2.10	0.06 - 0.10
S	0.00 - 0.60	0.06 - 0.10

To construct a pattern recognition model based on different morphologies, the initial knowledge base must be composed by specific ECG signals of each morphology. Unfortunately,

Fig. 1: Representation of the morphologies of the QRS complex used in this work: from left to right, we have qRs, RS, QS and rRs morphologies.



Fig. 2: Example of a synthetic PQRST cycle signal produced by the simulator.



labeling the ECG signals involves time and the involvement of a specialist, besides patients' permission. To mitigate this problem, a heartbeat simulator has been developed which can accurately approximate a real beat [15].

The simulator is characterized by a dynamic system based on three differential equations capable of generating realistic synthetic ECG signals. It is possible to specify the mean frequency and the standard deviation of the heart rate, the power spectrum of the RR time-series, the QRS complex morphology, Low Frequency (LF) and High Frequency (HF) bandwidth for heart rate variability along with the LF/HF ratio. Finally, the amplitudes and modulations of the PQRST cycle can also be specified, allowing a considerable variability for generated synthetic ECG signals.

Fig. 2 illustrates an example of a synthetic PQRST complex containing a QRS-complex with a qRs morphology.

III. ECG FEATURE EXTRACTION METHODOLOGY

Typical ECG signals are composed by many heartbeats. Each beat represents one ECG complex, or in other words, a PQRST cycle. Also, every ECG complex contains a QRS complex formed by the waves Q, R, and S. For our proposal, we need to find and extract the QRS-complex held in each ECG complex. The task of separating each QRS complex of an ECG signal is named QRS detection.

Among all approaches, Pan Tompkins[4] is a well-known technique to detect the QRS-complex. The Pan Tompkins algorithm identifies QRS complexes using digital analysis of amplitude, width, and slope of the ECG wave. Also, it uses a

patient-specific threshold for QRS peak detection, periodically adjusted to adapt to the changes in QRS morphology and heart rate.

After using Pan Tompkins algorithm for beat detection within the ECG signal, we obtain a set of QRS complexes, from which the features will be extracted. Our goal is to classify the morphology present in each QRS complex. Due to the significant morphological variability of the heartbeats, the process for feature extraction needs to be accurate and capture the correct information for each morphology, independent of amplitude levels, frequency sampling, and intrinsic noise of the ECG signal.

In our approach, we adopt three different functions that present a strong correlation with the structures of typical ECG morphologies presented in Fig. 1. The functions are Gaussian, Mexican Hat and Rayleigh, respectively defined below:

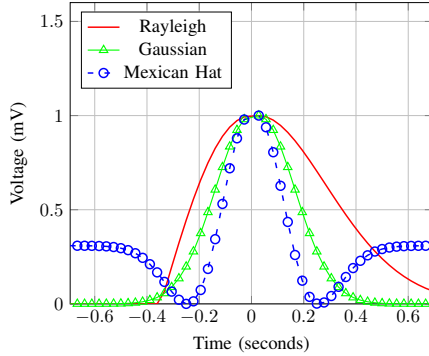
$$\mathcal{N}(x|\mu, \sigma^2) = \frac{1}{\sqrt{2\pi\sigma^2}} e^{-(x-\mu)^2/2\sigma^2}, \quad (1)$$

$$M(x|\lambda) = \frac{2}{\sqrt{3}\lambda\pi^{\frac{1}{4}}} \left(1 - \left(\frac{x}{\lambda}\right)^2\right) e^{-x^2/2\lambda^2}, \quad (2)$$

$$R(x|\lambda) = \frac{x}{\lambda^2} e^{-x^2/2\lambda^2}, \quad (3)$$

where μ and λ are location parameters and σ^2 is the variance/scale parameter of the functions. Each of these functions has similarities when compared with some ECG morphologies and, by combining them, it is possible to find patterns that identify a high number of morphologies. Fig. 3 shows the distribution of the cited functions.

Fig. 3: Illustration of the functions Rayleigh, Gaussian and Mexican Hat.



We build five different mathematical models by combining the individual functions: Gaussian, Mexican Hat, and Rayleigh. Each model is composed by two of these functions, according to Table II, the choice of functions was made in order to represent the largest number of morphologies, with the least number of models possible^{weslley}. For simplicity, we will call A/B, the first and second/functions used to build each model.

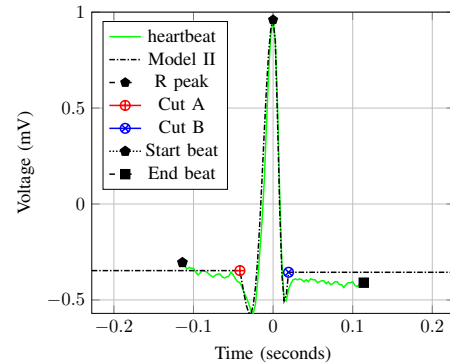
To compose models I and II, first we use each composition function to generate an individual signal model in which the number of points on the output window is linearly proportional to the number of points of the QRS complex

TABLE II: Composition of each proposed mathematical model.

Model	Mathematical Models	
	Function A	Function B
I	Gaussian	Gaussian
II	Mexican Hat	Mexican Hat
III	Rayleigh	(-1)Rayleigh
IV	(-1)*Rayleigh	Rayleigh
V	Rayleigh	Rayleigh

window. We do this process as follows: given the size of the QRS complex window w , we build two models, A and B, with length s_a and s_b , respectively. The length of the models (i.e., the number of points) is chosen from the range $[0.5w, 0.7w, 0.9w, 1.1w, \dots, 1.9w, 2w]$. Then, we remove the first/last k points of the models A and B, where k is chosen from $[0.1s, 0.2s, \dots, 0.5s, 0.6s]$. The process for selecting the parameters will be discussed in detail later. Besides that, we extend the models A and B by repeating their first/last value w times. After that, we select the peak with most significant absolute value for models A and B, and normalize them, forcing their peaks to have the same value. Finally, we merge the models overlapping both peaks. More specifically, the left part of the final model has the same distribution of the left part of the composition function A centered on their most significant peak, while the right part of the model has the same distribution of the right part of the function B, also centered in their most significant peak. Fig. 4 shows the final model merged from models A and B. From this point, for the sake of simplicity, we will omit the left and right parts of a signal are always related to its most significant peak.

Fig. 4: Fitting the original signal above extended version of model II. In green line: the heartbeat; Black pointed line: RCMF model; Cut A: cut point for function A. Cut B: cut point for function B. Start/end beat represent the limits of heartbeat window.



As illustrated by Figs. 5a, 5b, 5c and 5d, for the models III, IV, and V, the intersection of the two composition functions is the first point with zero value after/before respectively from the corresponding most significant peak of the functions A and B. The highest peaks from both functions are preserved

(note that they do not need to have the same value). The only procedure differences to build models I, II from III, IV, and IV is the way to merge the left and right parts. The first models have merged crossing their most significant values instead of the zero-crossing values.

Each composition function is tuned as follows. First, we define a range of parameters to experiment and construct the current model using the composition functions A and B, usually $\mu = 0$, σ^2 and $\lambda \in \{0.1, 0.5, 1, 1.5, \dots, 9.5, 10\}$. After building the model, it is necessary to find the R peak (for inverse R peaks like on QS morphology, we multiply the signal by -1) of a given heartbeat and the most significant peak of the model to normalize them in such a way that both maxima are at the same point. The construction of the proposed model guarantees that the size of the model is greater than or equal to the size of the QRS complex window. To correct this, we cut the remaining portion of the model based on a window of size equal to the QRS complex window, centered on the most significant value of the model.

At this point, both the signals, the heartbeat and the model, have the same length. To evaluate the selected parameters, we calculate the Mean Square Error (MSE) for the left/right part of the heartbeat/model. There is no difference in calculating the MSE separately for segmented parts of the ECG heartbeat, but since their morphology is not symmetric, it is possible to acquire some information concerning how differently the model fits different portions of the signal.

After the previous step, we have ten features composed by the evaluation errors of the mathematical models for each heartbeat piece. A normalization procedure is then applied for the feature set, to force the interval range $[0, 1]$. This procedure ensures that the features do not represent absolute errors, but relative indicators concerning the performance of the different models for fitting a given heartbeat.

Finally, we add a variable indicator concerning the sign of the R peak to the feature set. This indicator will help to decide between morphologies with opposite signs but with very similar relative errors. Algorithm 1 summarizes the proposed method.

IV. RELATED WORK

Prevention of death by heart disorders is an essential field in medicine. The advances of computer-aided diagnosis propel different works to detect/prevent such diseases. Among all approaches, heartbeat shape recognition has shown promising results when applied to identify a variety of heart disorders. Wavelet-based approaches have been one of the first family of techniques proposed for identifying heartbeat morphologies. In Martínez et al. [14], a Wavelet-based ECG delineator was proposed to deal with motion artifacts, muscular noise, baseline wandering, and changes in the QRS morphology. In that work, the morphology of QRS complexes depends on the number of negative/positive peaks, which are governed by thresholds, at scales $2^1, 2^2, 2^3, 2^4, 2^5$ related to filtered versions of the ECG signal [14]. However, detecting peaks is a task very sensitive to noise presence. Another common

Algorithm 1 *Feature extraction via residuals from modeling with composition of mathematical functions (RCMF)*

Input: QRS complex.

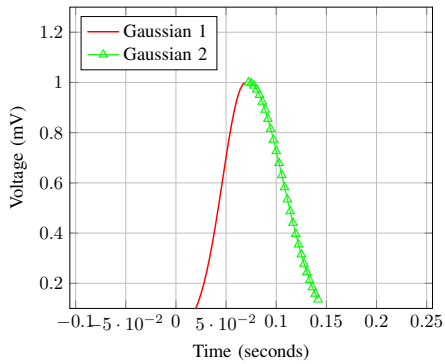
Output: the best found MSE (left and right parts) for each mathematical model. Original sign of R peak.

- 1: **for** each function in Eq. (1), Eq. (2) and Eq. (3) **do**
 - 2: **for** each parameter set $(w, s, k, \lambda, \mu, \sigma^2)$ **do**
 - 3: Build the models A and B from composition functions A and B and QRS window of size w .
 - 4: Remove the first/last k points on the models A and B .
 - 5: Repeat the first/last w points on the models A and B .
 - 6: Normalize the models A and B .
 - 7: Combine the models by overlapping their most significant peak peaks for models I and II and preserving both peaks for models III, IV and V.
 - 8: Match the most significant value of the final model and the inputted QRS complex.
 - 9: Cut the remaining points on the final model to build a model with window of size w .
 - 10: Find the most significant peak of the final model.
 - 11: Calculate the MSE from left/right part of the model/heartbeat matching the most significant peak of the final model and the R peak of the QRS complex.
 - 12: **end for**
 - 13: Select the best MSE (sum of the MSE of left and right parts) among all tested possibilities.
 - 14: **end for**
 - 15: Calculate the sign of the R peak.
-

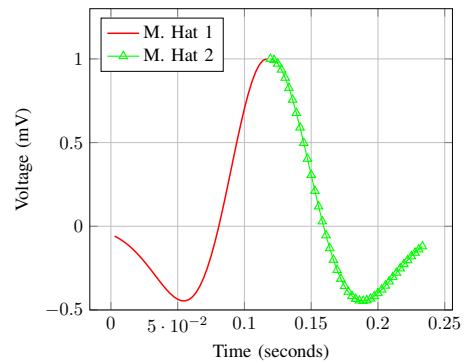
wavelet approach is to consider Daubechies wavelet (db1) to extract features according to Mar et al. [13]. As in [17], we have opted to use a 3-level decomposition to build a 23-feature array.

Later, statistical ECG descriptors were proposed in [3, 19], both based on the second, third, and fourth-order cumulants, with robustness to additive noise and capable of extracting information for nonlinear behavior. On the other hand, additional assumptions are needed, like a zero mean of the heartbeat signal. As in [17], each heartbeat was split into five bins and had their kurtosis and skewness extracted, resulting in a 10-feature array.

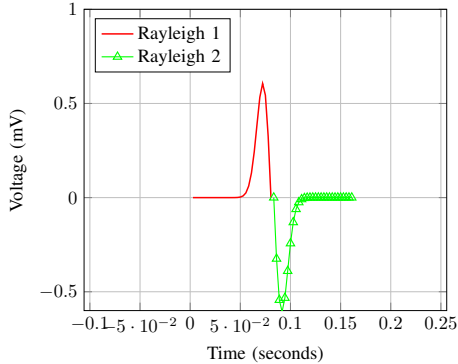
Concomitantly, [16] presented a curve fitting methodology for on-line heartbeat type recognition. After the QRS detection, the heartbeat was fitted using Hermite basis functions, which have the coefficients extracted and applied as features to characterize the shape of the signal. The main idea of this work is based on [10], which considers the similarity of the forms between fitted Hermite polynomials and QRS complexes. Unfortunately, it is possible to insert unusable features, since not all coefficients need to represent QRS morphologies well.



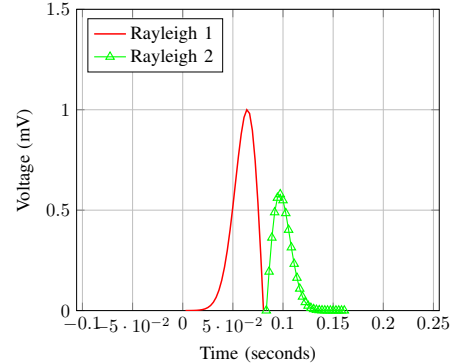
(a) Model built upon two Gaussian functions.



(b) Model built upon two Mexican hats.



(c) Model built upon two Rayleigh functions.



(d) Model built upon two Rayleigh functions.

Fig. 5: Mathematical models built using composition functions. The mathematical model IV is identical to model III, but its peaks are inverted. Note that model V differs from III only by the signal of the Rayleigh functions.

Moreover, many other approaches were proposed to classify arrhythmia. The first one is the 1D-local binary patterns (a variant of 2D-local binary pattern [8]) where each point of the heartbeat is compared with the neighbors producing a binary code. The histogram of the frequency of each binary pattern is used as a feature. The original work proposes an 8-neighbor 1D-LBP built 59-dimensional descriptor for a 180-dimensional heartbeat [17]. Secondly, in [6], an ensemble of SVM's with multiple random projections was applied to heartbeat classification. The features can be understood as multiple independent groups of random features. In our work, we reproduce the author's experiment using 15 classifiers with 50 features for each projection and using the majority vote to predict the classes. Finally, Mondéjar-Guerra et al. [17] recently proposed a morphological descriptor of the PQRST complex based on four windows. For a heartbeat with a window size of 180 samples (500ms) (centered on the R peak), the morphological descriptor is calculated using the Euclidean distance between the R peak and the points below:

- 1) $\max(\text{beat}[0:40])$
- 2) $\min(\text{beat}[75:85])$
- 3) $\min(\text{beat}[95:105])$
- 4) $\max(\text{beat}[150:180])$

After that, all features are normalized between 0 and 1. Nevertheless, all of these approaches are severely affected by

noise incidence.

Finally, many deep neural networks were proposed showing promising results [21, 24]. In this work, we reproduce the CNN 1D network at [21], with seven blocks of convolutional layers (128 filters, width 5), max-pooling, and dropout (rate=0.5). In the end, a global average pooling, 3 Full connected layers with (256/128/64), and softmax. ^{wesley}

V. DATASET AND PRE-PROCESSING

We apply a pre-processing step before extracting features from the available data. Following most of the previous works, for each signal we remove the baseline. We use a high order (10) polynomial to calculate our baseline. Then, we subtract it from the original signal. Similarly to [17], we have opted not to add any other noise filter or modification to preserve most of the original signal.

After extracting the heartbeats, we select the QRS segment as 71 data points around the R peak (31 points before and 35 ones after). Since the data sample rate is 360 Hz, a window of 71 points gives us approximately 200 ms, which is long enough to cover all the QRS complexes experimented in this work.

A. Artificial dataset

Using the previously described ECG data simulator, 10 synthetic signals were created for the morphologies qRs, RS,

QS, and rRs, composing a total of 40 signals with varying amplitudes and durations, according to Table I. The frequency of the signals was set at 360 Hz, with the heart rate ranging from 60 to 100 beats per minute and LF/HF ratio of 0.5 and approximately 2 hours in duration. For each signal, we apply the Pan Tompkins method to extract 25 heartbeats, which had the P and Q waves removed, leaving only the QRS complex. This results in a total of 1000 heartbeats, 250 for each morphology. For each beat, a window of size 35 samples centered around its R peak was used to extract the QRS complex.

B. MIT-BIH Dataset

The MIT-BIH Arrhythmia dataset contains 48 half-hour excerpts of two-channel ambulatory ECG recordings obtained from 47 subjects studied by the BIH Arrhythmia Laboratory between 1975 and 1979. To build our test dataset, we select fourteen subjects (100-lead 1, 100-lead 2, 101-lead 1, 103-lead 1, 105-lead 2, 106-lead 1, 108-lead 2, 111-lead 2, 215-lead 1, 116-lead 2, 117-lead 1, 219-lead 1, 219-lead 2, 121-lead 2, 223-lead 2, 123-lead 2) that contain the morphologies qRs, RS, QS, and rRs. Then, we apply the Pan Tompkins method to extract a set of heartbeats for each subject/morphology class. After that, the extracted QRS complex windows with 71 samples, or approximately 200ms, were manually labeled by a specialist, forming a dataset with 240 QRS complexes (60 for each morphology).

VI. EXPERIMENTAL RESULTS

To investigate the efficiency of the proposed features, we conducted two experiment designs that aim to compare our proposed work and other standard feature extraction techniques used on ECG signal classification.

In the first one, we assessed the efficiency of all feature extraction methods using only the simulated data provided by the synthetic generator. We randomly selected 2/3 of the instances for training and 1/3 for testing, ensuring that QRS complexes of the same time-series must be present only on training or testing set, but not on both at the same time. We chose Support Vector Machine (SVM) as the learning model, with the hyperparameters tuned following a 5-fold cross-validation in a grid-search procedure. For the hyperparameter search space, we chose $C \in \{2^{-1}, 2^{-1}, 2^{-1}, \dots, 2^{12}, 2^{15}\}$ and $\gamma \in \{2^{-15}, 2^{-13}, 2^{-11}, \dots, 2^1, 2^{13}\}$ for the Gaussian kernel, and $C \in \{2^{-1}, 2^{-1}, 2^{-1}, \dots, 2^{12}, 2^{15}\}$ for the linear kernel. The experiment was repeated 20 times.

To promote a fair comparison, we propose some adaptations for each approach when necessary. At first, since the morphological descriptor by Mondéjar-Guerra et al. [17] was designated for a heartbeat with length 180 samples (500ms) instead of 71 (~200ms), a rescale interpolation was applied to ensure the correct length. Besides that, the original methodology was designated for the whole heartbeat (including the P and T waves) choosing 4 regions to extract their features. In this work, we set the first and four regions on the extremities, and move the second and third regions, both with window

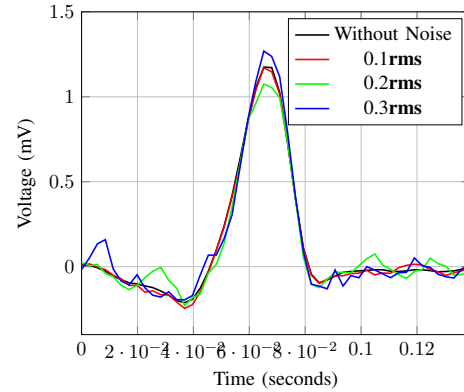


Fig. 6: Noise levels of a real heartbeat.

size of 10 samples along the time axis in opposite directions, skipping the same time of their window. Finally, we repeat this procedure increasing their window(second and third fuducial regions) size for 20, 30 and 40.

The original approach of Hermite Polynomials extends the QRS complex by adding 45 zero values to each of their extremities. Then, all QRS complexes are linearly normalized in the range $[-1, 1]$, and finally, the mean level of the first and the last data points is subtracted. We choose not apply this preprocessing step, since, in our preliminary experiments, it achieved poor results.

For the wavelet approach by Martínez et al. [14], the hyperparameter α was tuned within the values $[0.4, 0.5, 0.55, 0.6]$. This hyperparameter represents a threshold to identify real peaks instead of noise. The remaining methods were used without any modifications. We emphasize that only the artificially labeled data were used to select the hyperparameters.

It is interesting to note that according to Table III, all feature extraction methods achieve a good performance. In fact, only the 1D-LBP method had an accuracy lower than 90%. This finding confirms our initial hypothesis that artificial data can be learned by well-known heartbeat feature extraction methods.

TABLE III: Test results with artificial data.

Methods	Accuracy
Mondéjar-Guerra et al. [17]	0.980 ± 0.015
Wavelets Martínez et al. [14]	0.930 ± 0.030
Wavelets Mar et al. [13]	0.981 ± 0.054
Random Projection	1.000 ± 0.000
RCMF	0.997 ± 0.003
1D-IBP	0.898 ± 0.035
Hermite Polynomial	0.961 ± 0.051
1D CNN	0.982 ± 0.031
High Order Statistics	0.991 ± 0.018

The second experiment consists of using the artificial data to train the models and then evaluate them using the real data. We tuned all parameters using a 5 k-fold cross-validation with the artificial data set. Besides that, we repeat the experiment 20 times. To make the artificial data as more realistic as possible, for each extracted heartbeat, we repeat the experiment

adding a Gaussian noise with mean 0 and variance within the values $[0, 0.2rms(s), 0.3rms(s), 0.4rms(s)]$, where $rms(s)$ represent the root mean square level of the heartbeat. Fig. 6 illustrates the noise levels considered in this experiment.

Initially, we expected that all methods would have similar performance on the first and second experiments. However, as shown in Table IV, the feature sets obtained by wavelets and 1D-LBP achieved a poor performance in the second experiment when compared to the first experiment. Thus, we can hypothesize that these methods cannot handle slight differences between training and test sets. For instance, the wavelet features are based on peak detection, being therefore very sensitive to noise addition.

Apart from this slight discordance, the other methods performed well with accuracy greater or equal than 70%, including the other wavelet approaches. As expected, the artificial noise on the training data set provided a significant impact on the performance of the methods. It can be noticed that in most cases there were improvements in the accuracy for the 1° and 2° noise levels, possibly indicating that those noisy artificial signals are better approximations of real heartbeats with muscle noise.

It is important to note that Hermite polynomial and RCMF (our approach) acquired the best results among all the techniques. Both methodologies are based on fitting curves, which explain why they can better recognize the shape of the heartbeats. Our approach is the best in 3 of 4 scenarios, and it has obtained equal statistical results in one. This finding reinforces the efficiency of the proposed method. To support this, we have used the Kolmogorov-Smirnov test to verify whether two empirical data distributions are the same. In our experiments, it was used to compare pairs of classifiers and assess if the performance of any classifier is significantly different. Table V shows the results for our approach and Hermite Polynomials, for all noise levels.

According to the performed Kolmogorov-Smirnov test, we cannot reject the null hypothesis (two samples are drawn from the same distribution) if the p-value is greater than 0.05, which means that the performance of two models is significantly different. Considering this definition, we can verify that the RCMF approach significantly outperformed Hermite polynomial in the first 3 of 4 scenarios and it has statistically equal results on the other one. In summary, RCMF constitutes a valid alternative to other standard approaches, since they present a better or equal accuracy.

VII. CONCLUSION

Early detection of cardiovascular diseases (CVD) is a relevant field in medicine. The current approaches have many drawbacks, such as being noise sensitive or presenting poor generalization on unseen data. To overcome those issues, we proposed a new method, named feature extraction via residuals from modeling with composition of mathematical functions (RCMF), for the classification of the QRS morphology in ECG signals.

Based on the results obtained from computational experiments, we have verified that the RCMF approach achieved better accuracies when compared to other well-known feature extraction techniques for heartbeat classification. Additionally, we proposed new labels for some records of the MIT-BIH Arrhythmia database.

Future work may include new compositions of functions, like beta, triangular and bimodal distributions, aiming to extract information for new morphologies.

ACKNOWLEDGMENT

This work was supported by Coordination for the Improvement of Higher Education Personnel (CAPES), Brazilian Research Council, CNPq (Grant n. 426002/2016-4), and Ceara State Foundation for the Support of Scientific and Technological Development (BP3-0139-00284.01.00/18).

REFERENCES

- [1] Nourhan Bayasi, Temesghen Tekeste, Hani Saleh, Ahsan Khandoker, Baker Mohammad, and Mohammed Ismail. Adaptive technique for p and t wave delineation in electrocardiogram signals. In *2014 36th Annual International Conference of the IEEE Engineering in Medicine and Biology Society*, pages 90–93. IEEE, 2014.
- [2] Saurav Chatterjee and Nisarg Changawala. Fragmented qrs complex: a novel marker of cardiovascular disease. *Clinical cardiology*, 33(2):68–71, 2010.
- [3] Gael De Lannoy, Damien François, Jean Delbeke, and Michel Verleysen. Weighted svms and feature relevance assessment in supervised heart beat classification. In *International Joint Conference on Biomedical Engineering Systems and Technologies*, pages 212–223. Springer, 2010.
- [4] Aykut Diker, Engin Avci, and Mehmet Gedikpinar. Determination of r-peaks in ecg signal using hilbert transform and pan-tompkins algorithms. In *2017 25th Signal Processing and Communications Applications Conference (SIU)*, pages 1–4. IEEE, 2017.
- [5] Joao Paulo do Vale Madeiro, Elves Mauro Boa Esperanca dos Santos, Paulo Cesar Cortez, John Hebert da Silva Felix, and Fernando Soares Schlindwein. Evaluating gaussian and rayleigh-based mathematical models for t and p-waves in ecg. *IEEE Latin America Transactions*, 15(5):843–853, 2017.
- [6] Huifang Huang, Jie Liu, Qiang Zhu, Ruiping Wang, and Guangshu Hu. A new hierarchical method for inter-patient heartbeat classification using random projections and rr intervals. *Biomedical engineering online*, 13(1): 90, 2014.
- [7] Marek Jastrzebski, Jerzy Wiliński, Kamil Fijorek, Tomasz Sondej, and Danuta Czarnecka. Mortality and morbidity in cardiac resynchronization patients: impact of lead position, paced left ventricular qrs morphology and other characteristics on long-term outcome. *Europace*, 15(2):258–265, 2012.

TABLE IV: Performance comparison for all the evaluated feature extraction methods.

Method	Without Noise	0.1rms(x)	0.2rms(x)	0.3rms(x)
Mondéjar-Guerra et al. [17]	0.777±0.048	0.728±0.019	0.691±0.087	0.676±0.029
WaveletsMartínez et al. [14]	0.641±0.009	0.474±0.014	0.443±0.071	0.587±0.003
Wavelets Mar et al. [13]	0.867±0.002	0.765±0.001	0.867±0.124	0.667±0.100
1D-LBP	0.217±0.091	0.546±0.026	0.360±0.015	272±0.037
Random Projection	0.873±0.006	0.870±0.049	0.862±0.015	900±0.003
RCMF	0.991±0.013	0.995±0.001	0.989±0.003	0.950±0.048
Hermite Polynomial	0.961±0.013	0.971±0.011	0.975±0.028	0.949±0.032
1D CNN	0.931±0.014	0.921±0.022	0.922±0.026	0.919±0.017
High Order Statistics	0.707±0.017	0.707±0.019	0.786±0.008	0.711±0.005

TABLE V: Kolmogorov-Smirnov test for Hermite Polynomials and RCMF.

Noise level variance	KS statistic	p-value
0	9.00000000	0.000000036
0.1rms	0.94999999	0.000000004
0.2rms	0.69999999	0.000041504
0.3rms	0.25000000	0.497342335

- [8] Yılmaz Kaya, Murat Uyar, Ramazan Tekin, and Selçuk Yıldırım. 1d-local binary pattern based feature extraction for classification of epileptic eeg signals. *Applied Mathematics and Computation*, 243:209–219, 2014.
- [9] Mand JH Khidir, Victoria Delgado, Nina Ajmone Marsan, Martin J Schlij, and Jeroen J Bax. Qrs duration versus morphology and survival after cardiac resynchronization therapy. *ESC heart failure*, 4(1):23–30, 2017.
- [10] Martin Lagerholm, Carsten Peterson, Guido Braccini, Lars Edenbrandt, and Leif Sornmo. Clustering eeg complexes using hermite functions and self-organizing maps. *IEEE Transactions on Biomedical Engineering*, 47(7):838–848, 2000.
- [11] Tatiana S Lugovaya. Biometric human identification based on eeg, 2005.
- [12] Eduardo José da S Luz, William Robson Schwartz, Guillermo Cámara-Chávez, and David Menotti. Ecg-based heartbeat classification for arrhythmia detection: A survey. *Computer methods and programs in biomedicine*, 127:144–164, 2016.
- [13] Tanis Mar, Sebastian Zaunseder, Juan Pablo Martínez, Mariano Llamedo, and Rüdiger Poll. Optimization of eeg classification by means of feature selection. *IEEE transactions on Biomedical Engineering*, 58(8):2168–2177, 2011.
- [14] Juan Pablo Martínez, Rute Almeida, Salvador Olmos, Ana Paula Rocha, and Pablo Laguna. A wavelet-based eeg delineator: evaluation on standard databases. *IEEE Transactions on biomedical engineering*, 51(4):570–581, 2004.
- [15] Patrick E McSharry, Gari D Clifford, Lionel Tarassenko, and Leonard A Smith. A dynamical model for generating synthetic electrocardiogram signals. *IEEE transactions on biomedical engineering*, 50(3):289–294, 2003.
- [16] Farid Melgani and Yakoub Bazi. Classification of electrocardiogram signals with support vector machines and particle swarm optimization. *IEEE transactions on information technology in biomedicine*, 12(5):667–677, 2008.
- [17] V Mondéjar-Guerra, J Novo, J Rouco, M G Penedo, and M Ortega. Heartbeat classification fusing temporal and morphological information of ECGs via ensemble of classifiers. *Biomedical Signal Processing and Control*, 47:41–48, 2019. ISSN 1746-8094. doi: <https://doi.org/10.1016/j.bspc.2018.08.007>.
- [18] Navar Medeiros M Nascimento, Leandro B Marinho, Solon Alves Peixoto, João Paulo do Vale Madeiro, Victor Hugo C de Albuquerque, and Pedro P Rebouças Filho. Heart arrhythmia classification based on statistical moments and structural co-occurrence. *Circuits, Systems, and Signal Processing*, pages 1–20, 2019.
- [19] Stanislaw Osowski and Tran Hoai Linh. Ecg beat recognition using fuzzy hybrid neural network. *IEEE Transactions on Biomedical Engineering*, 48(11):1265–1271, 2001.
- [20] Jeanne E Poole, Jagmeet P Singh, and Ulrika Birgersdotter-Green. Qrs duration or qrs morphology: what really matters in cardiac resynchronization therapy? *Journal of the American College of Cardiology*, 67(9):1104–1117, 2016.
- [21] B Pyakillya, N Kazachenko, and N Mikhailovsky. Deep learning for eeg classification. In *Journal of physics: conference series*, volume 913, page 012004. IOP Publishing, 2017.
- [22] Manoj Kumar Senapati, Mrutyunjaya Senapati, and Srinivasu Maka. Cardiac arrhythmia classification of eeg signal using morphology and heart beat rate. In *2014 Fourth International Conference on Advances in Computing and Communications*, pages 60–63. IEEE, 2014.
- [23] Tomás Teijeiro, Paulo Félix, Jesús Presedo, and Daniel Castro. Heartbeat classification using abstract features from the abductive interpretation of the eeg. *IEEE journal of biomedical and health informatics*, 22(2):409–420, 2016.
- [24] Özal Yıldırım, Paweł Pławiak, Ru-San Tan, and U Rajendra Acharya. Arrhythmia detection using deep convolutional neural network with long duration eeg signals. *Computers in biology and medicine*, 102:411–420, 2018.
- [25] Maxime Yochum, Charlotte Renaud, and Sabir Jacquir. Automatic detection of p, qrs and t patterns in 12 leads eeg signal based on cwt. *Biomedical Signal Processing*

and Control, 25:46–52, 2016.